AD NUMBER: AD0140220
LIMITATION CHANGES
TO: Approved for public release; distribution is unlimited.
FROM: Distribution authorized to U.S. Gov't. agencies and their contractors; Administrative/Operational Use; 2 Mar 1948. Other requests shall be referred to Ballistic Research Laboratories, Aberdeen Proving Ground, MD 21005.
AUTHORITY
BRL ltr dtd 22 Apr 1981

[redacted]

BALLISTIC RESEARCH LABORATORIES

REPORT NO. 661

Charts for the Exterior Ballistics of Mortar Fire Based on the Square Law of Drag

S. J. ZARODNY

D. M. BROOKS

ABERDEEN PROVING GROUND, MARYLAND

[redacted]

BALLISTIC RESEARCH LABORATORIES

REPORT NO. 661

Charts for the Exterior Ballistics of Mortar Fire Based on the Square Law of Drag

S. J. ZARODNY
D. M. BROOKS

PROJECT NO. TB3-0108 OF THE RESEARCH AND DEVELOPMENT DIVISION, ORDNANCE DEPARTMENT

2 MARCH 1948

ABERDEEN PROVING GROUND, MARYLAND

[redacted]

TABLE OF CONTENTS

BALLISTIC RESEARCH LABORATORIES

REPORT NO. 661

S.J. Zaroodny/D.M. Brooks
Aberdeen Proving Ground, Md.
2 December 1947

CHARTS FOR THE EXTERIOR BALLISTICS OF MORTAR FIRE BASED ON THE SQUARE LAW OF DRAG

ABSTRACT

Otto-Lardillon tables of exterior ballistics based on the square law of drag are extended and plotted in a form arranged for convenience in use in connection with mortar fire problems. The applicability of this method to the mortar fire problems is noted. The theory of the square law is reviewed. Methods for obtaining diverse differential corrections are given. Sufficient data are included for point-by-point construction of the trajectory.*

*This work is a revision and extension of the data presented in Chapter I, BRLM Report No. 434.

INTRODUCTION

It has been often felt that the development of mortar fire would proceed more certainly and rapidly if diverse exterior ballistic calculations for this fire could be made more widely and more frequently. For this reason a need was felt for a method of exterior ballistic calculations for mortar fire that would be not only correct but, particularly, very simple. Such a method is found in the well-known and old assumption that the drag on the shell varies simply as the square of the shell's velocity.

DISCUSSION

At first thought one may well feel suspicious toward the suggestion to use the square law of drag: for it is too reminescent of the attempts of the 18th and 19th century mathematicians to obtain an analytical solution of the exterior ballistic problem. This form of drag-velocity relationship was suggested by Newton before 1686; the mathematical treatment of the exterior ballistic trajectory subject to this law was given by Bernoulli in 1719 and Euler in 1753; in fact, the calculations on which the charts given in this report are based were published in 1842. Since then the approach to the exterior ballistic problem has undergone a fundamental change: now the drag-velocity relationship is generally established experimentally, and the trajectory is then determined by the numerical integration of its differential equations[1]. Nevertheless, there are several considerations that still commend the square law of drag, when in its proper place. We shall list these.

Firstly, of course, the square law of drag, if used, should be restricted to the subsonic range of velocities.[2] This limitation, however, still leaves a broad field. Practically all mortar fire (with the possible exception of the very latest shell) is well within the subsonic range. This circumstance characterizes not so much our present weapons, as the inherent tactical character of mortar fire, i.e., its relatively short range.

Secondly, numerical integration, though basically correct, is only as good as the data on which it is based. Determination of drag by firing constitutes essentially a double differentiation; therefore, the experimental data on drag are inherently limited in accuracy and difficult to obtain, and for that reason, are scant. In fact, up to the present time there is no drag function of a mortar shell obtained by firings. In absence of such a drag function the exterior ballistic calculations for mortar shell are usually made with the help of some drag function for artillery shell, notably the Gavre function. This procedure is employed

---

[1] To quote from Hayes' "Elements of Ordnance" (pp. 435 and 439): "While the impossibility of solving the ballistic problem in terms of explicit formulas is now recognized, this point of view is comparatively recent. The earliest study consisted in a search for such formulas. At that time, interest in exterior ballistics was largely academic, the subject being developed by mathematicans because they found it interesting, not because the results were needed for gunnery purposes. . . . . Long after these earlier conditions ceased to apply, they continued to exert a strong influence on the method of attack on the trajectory problem. . . . . Numerical integration . . . . .provides for perfect generality in the differential equations, thus allowing the introduction of the results of any experimental or mathematical developments as they may appear. . ."

[2] It was mainly the attempt to account for the behavior of the shell in the transsonic and in the supersonic range of muzzle velocities that troubled the early ballisticians.

merely because diverse tables for these functions are available; in fact, there are reasons to believe that the drag functions for artillery shell are not properly applicable to mortar shell. If we are to employ corrections, such as form-factors, for our calculations, we may just as well (and in fact, should prefer to) apply such corrections to a simpler method.

Thirdly, there are several reasons why we should expect the drag coefficient of mortar shell to be more nearly constant than the drag coefficient of the Gavre function:

a. Mortar shell is generally so well streamlined that the local shock waves (which constitute the compressibility effect) appear only when the velocity of sound is approached quite closely. There is some experimental evidence for this: models of 105mm T17 and T26 shell, and of 155mm T26, with various lengths of booms, have been measured in the Supersonic Wind Tunnel at Mach numbers of .45 (the lowest practicable), .60, .75 and .85 (corresponding to 950 fps), and the effects of the Mach number on the aerodynamic coefficients were found to be very small (in fact, barely significant). Also the shock waves, even with the bad-shaped T164 fuze, did not appear till Mach number of .85 was reached.

b. With mortar shell the skin friction, which does not rise suddenly near velocity of sound, constitutes a larger fraction of the total drag.

c. An additional reason favoring the use of the square law with mortar shell is that these shell, fired usually at high elevations, rapidly lose their velocity thru gravity, rather than thru drag alone; therefore, the effects of the transsonic range on the trajectory of these shell cease quicker, and are smaller, than with low-angle artillery fire.

Fourthly, it is natural to expect that the assumption of the square law of drag would considerably simplify all exterior ballistic calculations. However, it may be well to review just why this should be so:

a. From the point of view of dimensional analysis the square law of drag is the only possible form of drag-velocity relationship.. The deviation from this law has to be treated by allowing the dimensionless coefficient of proportionality, i.e., the drag coefficient K_D, in the dimensional expression for drag,[1]

$$(\text{drag})_{\text{lb-ft/sec}^2} = (\rho_{\text{lb/cu.ft}})\,(d_{\text{ft}})^2\,\left[K_D(v_{\text{ft/sec}})^2\right] \qquad (1)$$

to be a variable, i.e., effectively a function of velocity. It is surely a convenience to be able to think of K_D as a constant associated with the shell, as we would like the ballistic coefficient, or the form-factor, to be.

b. With the square law of drag (and with a corollary assumption that the air density ρ is constant) the differential equations of trajectory can be solved in terms of quadratures (even if these quadratures, unfortunately, are rather laborious to handle.)

c. From the practical point of view, however, the most important advantage of the square law of drag lies in the fact that it allows the representation of the relationship between four variables, viz., the range X, the muzzle velocity V, the elevation ϕ and a constant characterizing the shell, c, in a single chart. Generally, on a single chart (by drawing a family of curves, i.e., by representing a surface in the

[1] Here ρ is the air density and d the caliber.

three-dimensional space, or on a simple two-entry table) one can represent only a function of two variables; but the range of the shell, for instance, is a function of three variables: $X = X(V,\phi,c)$. To represent such a function it is necessary to have a bulky set of charts (or a set of tables) that would require laborious interpolation. With the square law of drag, however, it is possible to combine the three variables, X, V and c, into two groups of two, say $\mu(X,V)$ and $\eta(V,c)$, in such a way that between the three variables, μ, η and ϕ, there exists a relationship that can be represented on a single chart. Having ascertained the values of μ, η, ϕ from the chart, in order to obtain the value of either one of the three variables, X, V and c, as a function of μ and η, we have to make some additional calculations (for instance, to compute X from the given values of μ and V), but those are quite easy. It is interesting to note that the square law of drag appears to be the only physically plausible form of drag-velocity relationship that would allow such a representation.

On the other hand, in order to obtain the benefits of the mathematical simplification of the assumption of the square law of drag we have to make a corollary assumption, viz., that the air density ρ is a constant. Of course, this is not strictly true; large mortar shell at high elevations and very high velocity may reach an altitude as great as 10,000 ft., where the air density is reduced by as much as 28%. Fortunately, however, we do not have to assume strictly both a constant K_D and a constant ρ; we need to assume only a constant product $K_D\rho$. At higher altitudes, it is generally observed, the shell travles with a greater yaw[1], with a resultant increase in K_D; so that these two effects cancel each other to a certain extent. Inasmuch as normally we do not (as yet) allow for one of these two effects (the variation of the yaw-drag, as well as the resultant lift) along the trajectory, there does not seem to be much point in allowing for the other (the variation of air density). The residual effect, i.e., the variation of the product $K_D\rho$, from one trajectory to another, can be taken into account by allowing a variation of the form-factor, as is customary. It should be noted that in our method such a variation of the product $K_D\rho$ can be readily translated into an assumption of an air density that is "average" for the given trajectory.

The final argument in favor of the square law of drag is simply that it works, and in fact, often seems to work better than the Gavre function. We may note that because of its inherent simplicity, we would prefer the square law of drag (to the Gavre function) even if it were no better. Another point to keep in mind is that the present large dispersion of mortar fire often makes the distinction between various drag functions rather useless, so that the ease of computations remains the only practical criterion for comparing various drag functions. A review of some available data comparing the square law of drag with the Gavre function is given in Appendix V.

THEORY

The theory of the ballistic calculations with the square law of drag is given, for instance, in Cranz[2]. It is reviewed in Appendix I of this report.

---

[1] This fact, now tentatively explained by the theory of instability of spin, underlies the phenomena of short ranges and dispersion of mortar fire.

[2] C. Cranz, "Lehrbuch der Ballistik", 1st vol. (Aussere Ballistik), pp 140-144, 577-605 and 706 ff. A photolithoprint reproduction of the 5th edition (1925) is published (by Edwards Brothers, Ann Arbor, Mich) and distributed by authority of the Alien Property Custodian. An English translation of a less complete 2d edition (1921) is available, but apparently has no numerical tables.

Although the differential equations of the trajectory with the square law of drag are solvable in terms of quadratures, it will be noticed from Appendix I that these quadratures are quite cumbersome. A presentation of the numerical data is therefore necessary. Such presentation, the Otto-Lardillon tables, is given in Cranz. These tables are sufficient for solving the problems involving only the terminal data for the trajectory. There is also given one summital datum, the ratio of the maximum altitude to the range. Other summital data, viz., the range and the time of flight to the summit, unfortunately, are lacking. These Otto-Lardillon tables have been extended (from 75° to 90° elevation, and by provision of the needed summital data) and plotted, in a form arranged for the convenience of calculations, in the charts given in this report. The connection between the theory and the Otto-Lardillon tables, as well as the construction of our chart, is discussed in Appendix II of this report.

DESCRIPTION OF THE CHARTS

The large chart, Fig. 1, given in this report is sufficient for solving most mortar fire problems.

a. The ordinate on this chart is the dimensionless quantity

$$\eta = \sqrt{cV^2/g} \tag{2}$$

here V is the muzzle velocity, g is the acceleration of gravity and c is a constant characterizing the shell. This constant is defined by the statement that the deceleration of the shell due to drag at a velocity v is cv^2. Thus $\eta^2 = cV^2/g$ is simply the ratio of the deceleration due to drag at the muzzle velocity to the acceleration of gravity. Comparing the expression drag = cv^2 with (1), we readily see that

$$c = K_D \rho d^2/m \tag{3}$$

and has the dimension of reciprocal length[1]. Consistent units are assumed. The ordinate, η, indicates the importance of the drag, whether it be due to a poor projectile (large c) or to a high V. The bottom line on the chart, $\eta = 0$, shows the performance of the shell in vacuum.

b. The abscissa of the chart is the dimensionless quantity

$$\mu = 2gX_c/V^2 \tag{4}$$

where X_c is the range in consistent units[2]. This choice of the form of the function $\mu(X,V)$ shows the dependence of X upon ϕ and η most vividly, and also allows the interpolation to the limiting condition $\phi = 90°$, represented by the left-hand edge of the chart.

---

[1] If the air density ρ is in lb/ft^3, the weight of the shell m is in lbs, the caliber d should be in ft, and c comes out in ft^{-1}.

[2] In the following we use the same notation as on the chart, reserving the symbol X for the range in yards.

c. The main set of lines on the chart is that of the lines of constant elevation, ϕ. The coordinates μ and η together with the lines of ϕ suffice for most of the present-day mortar-fire problems, such as:

(1) Given V, ϕ and X, to find c: compute μ, locate point on chart, read η, compute $c = g(\eta/V)^2$.

(2) Given c, V and ϕ, to find X_c: compute η, locate point, read μ, compute $X_c = \mu V^2/2g$.

(3) Given c, V and X_c, to find ϕ: compute μ and η, locate point, read ϕ.

Since V enters in both μ and η, another procedure is advantageous in such problems when it is desired to determine V from given c, X and ϕ. Such problems can be solved either by trial-and-error, or use can be made of the thin lines of constant auxiliary variable ν, defined by

$$\nu = 2cX_c \tag{5}$$

Only a few of these lines are drawn on the chart. Additional lines can be easily drawn thru the small circles on the lines of ϕ: these circles represent the data from the Otto-Lardillon tables that are given for the round values of ν. Lines of ν are simple cubic hyperbolas given by $\eta^2\mu = \nu$.

TIME OF FLIGHT

The time of flight T, consistent with the theory, is given on the chart in terms of the dimensionless variable

$$\gamma = T\sqrt{gc}. \tag{6}$$

Many problems involving the time of flight can be solved by using this variable. These are essentially the problems of finding any two of the five variables, T, X, V, ϕ and c when the other three are given.

However, in the applications of value of T so computed (for instance, in comparing this computed value with the value observed in the firings) a caution is necessary. A point on the chart fixes the relationship between four of these five variables, and therefore the measurement of the fifth constitutes an over-determination. Generally the fifth datum will not check with the others. In fact, there are reasons why some discrepancy is to be expected, viz.:

a. The observed values of X and T include the effect of wind. The wind, particularly at high elevations, affects X considerably, but T only negligibly.

b. Euler-Otto-Lardillon theory (and for that matter, most of the present-day exterior ballistic computations) does not consider the effect of lift (the kiting effect, resulting from the fact that shell does not actually fly exactly nose-on and that there are therefore forces acting upon the shell that are perpendicular to trajectory). The yawing shell oscillates in such a manner (and about such a mean angular position) that on the average it always points above the trajectory. The effect of such a steady component of yaw is literally to lift the shell, and therefore, always to increase T. The effect upon X, however, is relatively small: for along the ascending branch of the trajectory the lift pushes the shell back, while on the descending branch the shell is pushed forward.

A complete answer to a mortar fire problem should include in some way an indication of this inherent discrepancy between X and T. Study of this discrepancy is one method from which we can find the importance of the lift and wind effects; in fact, one of the principal reasons for this work is to provide a method of computations by which these effects could be evaluated. At the present time perhaps the best way of handling this discrepancy is to cite two values of c, both corresponding to the same point on the chart but one used for estimating the range in connection with η and formula (2), as discussed above, and another used for estimating the time of flight in connection with γ and formula (6); to distinguish these two values, they might be denoted c_x and c_t. The discrepancy can be referred to as "the X-T discrepancy" and can be expressed in per cent, as

$$\text{X-T discrepancy} = c_x/c_t - 1 \qquad (7)$$

here c_x is determined from (2) as $c_x = g(\eta/V)^2$; to determine c_t, we read the value of γ from the chart (at the same point) and compute, from (6), $c_t = (\gamma/T)^2/g$.

The presentation of the data on the time of flight could have been done in a number of ways. For instance, the rendition of T dimensionless (which is the usual way of generalizing a variable) can be done by multiplying it by any one of several suitable combinations of the relevant variables: X_c (L), V (LT^{-1}), g (LT^{-2}) or c (L^{-1}).

a. The variable used in Otto-Lardillon tables is $T\sqrt{g/X_c}$; that selection is not particularly fortunate, for at high elevations the range X is very sensitive to the wind, and the experimental value of X_c (on which one perforce has to base the calculations) contains the wind effect.

b. The form in which we present the T (i.e., $\gamma = T\sqrt{gc} = (T\sqrt{g/X_c})(\sqrt{2cX_c})/\sqrt{2}$) still depends upon a "fudged" c_t; on the other hand, this form allows the simplest way of determining this c_t, and this c_t is one variable into which this discrepancy can be most conveniently "swept", or to which this discrepancy can be ascribed.

c. Perhaps a more unequivocally defined variable would be the combination Tg/V, since V is usually known accurately. Using such a variable we would find the intersection of a line representing its appropriate value with the line of ϕ, and would define c_t thru the new η; i.e., instead of using two different values of c at one point of the chart, we would locate two points on the chart, one for X and one for T (for an example of such calculation see second paragraph on page 28, Appendix IV). Variable Tg/V can be computed as γ/η.

d. A number of other ways of handling T and the wind-and-lift-effect discrepancy can be worked out to suit any particular problem.

DIFFERENTIAL CORRECTIONS

The charts can also yield a number of differential corrections, viz., the following:

$$\partial X_c/\partial V = (X_c/V)(2 - k_1\eta/\mu)$$

$$\partial X_c/\partial \phi = - X_c k_2/\mu$$

$$\partial X_c/\partial c = (X_c/c)k_1\eta/2\mu$$

$$\partial T/\partial V = k_3/g$$

$$\partial T/\partial \phi = k_4 T/\gamma$$

$$\partial T/\partial c = (T/2\gamma c)(k_4\eta - \gamma)$$

$$\partial X_c/\partial W_x = T - (X_c/V)(2\cos\phi - k_1\eta\cos\phi/\mu + k_2\sin\phi/\mu)$$

$$\partial T/\partial W_x = (k_4 T/\gamma V)\sin\phi - (k_3/g)\cos\phi$$

$$\partial Z_c/\partial W_z = T - X_c/v\cos\phi$$

and, of course, $\partial X_c/\partial W_z = \partial Z_c/\partial W_x = \partial T/\partial W_z = 0.$

The formulas for these differential corrections are summarized also on the charts (in common units, i.e., using the ballistic coefficient C_s instead of c, and range X in yards instead of X_c in feet). The derivation of these corrections is given in Appendix III. The k's contained in these formulas are the following dimensionless partial derivatives, all positive and in the units of the charts, and obtainable graphically:

$k_1 = |(\partial\mu/\partial\eta)_\phi|$

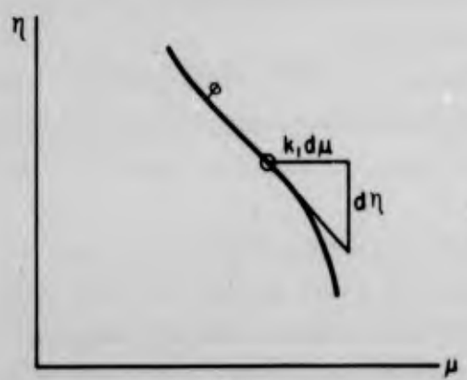

$k_3 = (\partial\gamma/\partial\eta)_\phi$

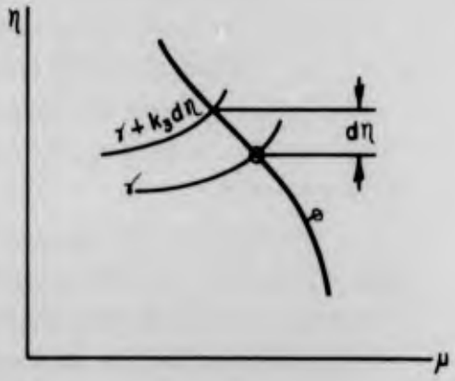

$k_2 = |(\partial\mu/\partial\phi)_\eta|$

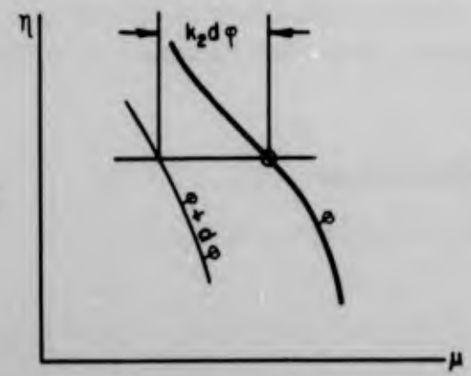

$k_4 = (\partial\gamma/\partial\phi)_\eta$

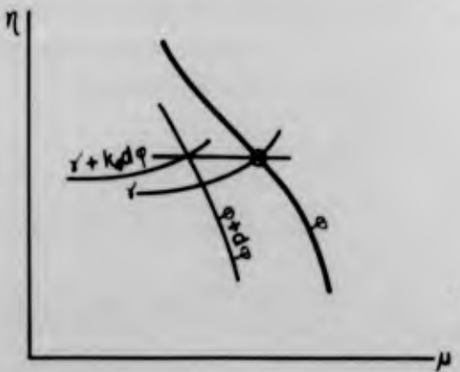

COMMON UNITS

The formulas cited above hold in any set of consistent units. One such set is: seconds for T, fps for V, ft for X_c and ft^{-1} for c. However, in ordnance practice the range X is usually expressed in yards, rather than in feet, and the shell is characterized by a ballistic coefficient, rather than by c. Accordingly, some minor modification of these formulas is convenient.

The ballistic coefficient of the shell is customarily denoted by a capital C with a subscript that indicates on which one of the several standard shell, or of the several tabulated drag functions, the calculations are based; for instance, subscript 1 refers to the well-known Gavre function. The drag coefficients of several artillery shell drag functions are shown, as functions of the Mach number in the subsonic range, in the insert on the large chart. The ballistic coefficient of any shell is defined by an expression such as

$$C_1 = m/i_1 d^2,$$

where m is the weight of the shell in lbs, d is the caliber in inches and i (with the same subscript as C) is the "form-factor", defined as the ratio of the drag coefficient K_D of our shell to the drag coefficient of the standard shell. The use of the ballistic coefficient implies the assumption that this ratio is the same at all velocities. For the standard shell itself, of course, i = 1.

In our case we choose the subscript s (for "square") and as the standard shell we take, for convenience, a hypothetical shell with $K_D = 0.1$; therefore, i_s is simply $10\ K_D$, and

$$C_s = m/i_s d^2 = m/(K_D/0.1)d^2 = m/10K_D d^2. \qquad (3')$$

Our formulas are then modified as follows:

a. Since X_c in feet is 3X (where X is the range in yards) formula (4) becomes

$$\mu = 2(32.17)(3X)/V^2 = 193\ X/V^2 \qquad (4')$$

b. Substituting in formula (3) for d (in feet) the expression d/12, where d is now in inches, we have

$$c = K_D \rho d^2/144m = (10\ \rho/144)/(m/10\ K_D d^2) = (10\ \rho/144)/C_s \qquad (3'')$$

and furthermore, substituting for ρ its standard value at ground, $\rho = .0751$ lb/cu ft,

$$c = 1/19{,}174\ C_s \qquad (3''')$$

c. Formula (2) becomes

$$\eta = V/\sqrt{19174\ C_s\ 32.15} = .001274\ V/\sqrt{C_s} = V/785.1\ \sqrt{C_s} \qquad (2')$$

d. Formula (6) becomes

$$\gamma = T\sqrt{32.15/19174\ C_s} = T/24.42\sqrt{C_s} \qquad (6')$$

e. Formula (5) becomes

$$\nu = 2(1/19174\ C_s)(3X) = X/3196\ C_s \qquad (5')$$

f. And finally, formula (7) becomes

$$\text{X-T discrepancy} = C_{st}/C_{sx} - 1. \qquad (7')$$

USES AND LIMITATIONS OF THE CHARTS

A number of detailed examples of use of these charts is given in Appendix IV[1]. In Appendix IV there is also given a discussion of the point-by-point construction of the trajectory from the charts (rather than by carrying the quadratures of Appendix I). Such construction might be desired in the forthcoming work on mortar fire, particularly for the application of McShanes's method of estimating the effect of the lift (and of stability of the shell) upon the range. The method of breaking the trajectory in separate arcs also lends itself to what is analogous to Mayevsky's method: for instance, the trajectory of a mortar shell starting at say 1200 fps may be carried out by numerical integration, or other means, with an appropriate drag function, a short distance into subsonic range, and thereafter the square-law trajectory may be used.

The charts are obviously limited in accuracy: firstly, because of the simplifying assumptions made; secondly, because of graphical presentation on a limited scale; and thirdly, they contain most of the inaccuracies of the original Otto-Lardillon tables.

Large contact reproductions of these charts are available in this Laboratory and may be secured upon request.

Serge J. Zaroodny

Dorothy M. Brooks

[1] A reader interested only in the practical use of the chart can omit reading Appendices I, II and III.

APPENDIX I

REVIEW OF THE THEORY OF THE SQUARE LAW OF DRAG

Consider the vector representing the instantaneous velocity of the shell. Let its length be v, and its inclination to the horizontal, θ. The angle θ is positive for the ascending branch of the trajectory, equals zero at the summit, and is negative for the descending branch. The rate of change of this vector, i.e., the deceleration of the shell, is the sum of the acceleration of gravity g, acting downward, and of the deceleration due to drag, which acts in the direction opposite to v (it being assumed that the shell always flies nose-on, so

that the lift can be neglected). The latter deceleration is generally written as $K_D \rho d^2 v^2/m$, where m and d (mass and caliber of the shell) are constant, and K_D and ρ (the drag coefficient and air density) may vary. We are concerned with the simpler case, when the product $K_D \rho$ is constant. Let $c = K_D \rho d^2/m$; then the deceleration due to drag is cv^2, c being a constant that characterizes the shell. From the sketch we see that the change in v during the time interval dt can be given, for instance, by the equations

$$d\theta = - g\, dt \cos\theta / v \qquad \text{(radians)} \tag{1}$$

$$\text{and } d(v\cos\theta) = - cv^2 \cos\theta\, dt \tag{2}$$

When we eliminate dt from these equations, by dividing (2) by (1), we obtain the differential equation of the hodograph of the trajectory (i.e., of the curve described by the end of the vector v in our sketch, in polar coordinates).

$$d(v\cos\theta)/d\theta = cv^3/g, \tag{3}$$

This equation is a necessary preliminary to the computation of the trajectory (or of the terminal data). In this simple form (due to our assumption) this differential equation is soluble by the separation of the variables and a simple quadrature. Multiplying (3) by $(g/c)d\theta/v^3\cos^3\theta$, we have

$$(g/c)d(v\cos\theta)/(v\cos\theta)^3 = d\theta/\cos^3\theta,$$

which can be integrated, giving the actual hodograph equation

$$-g/2cv^2\cos^2\theta = \int d\theta/\cos^3\theta - C \qquad (4)$$

The integral on the right-hand side of (4), when evaluated between 0 and θ, is denoted by ξ:

$$\xi(\theta) = \int_0^\theta \sec^3\theta\, d\theta \qquad (5)$$

This is an odd function of θ, positive for the ascending branch, = 0 at the summit and negative for the descending branch. It has an explicit form, $.5(\tan\theta \sec\theta + \ln\tan(\theta/2 + \pi/4))$, and is tabulated in the extensive table 8b of Cranz's (pp. 585-605). A brief table of ξ is given in this Appendix.

The constant of integration C (not to be confused with the ballistic coefficient C_s), defined with these limits of the ξ-integral, is a convenient parameter of the hodograph and of the trajectory. It can be determined, by writing the hodograph equation as

$$C = \xi(\theta) + g/2cv^2\cos^2\theta, \qquad (4')$$

whenever both v and θ are known (for a given c). In particular, for the initial (muzzle) conditions, when v = V and $\theta = \phi$,

$$C = \xi(\phi) + g/2cV^2\cos^2\phi. \qquad (4'')$$

It is interesting to note that C is completely determined by the summital conditions, when $v = v_s$ and $\theta = \xi(\theta) = 0$; for then $C = g/2cv_s^2$. The summit is therefore a convenient reference point of the trajectory. Any one C may refer to any number of trajectories with different V's and ϕ's, as long as the pairs V and ϕ satisfy (4''). With the parameters c and C, the hodograph equation determines v for any θ:

$$v^2 = g/2c\cos^2\theta(C - \xi(\theta)) \qquad (6)$$

From (6) we may notice, incidentally, that there is an upper limit, β, of θ, determined by $\xi(\beta) = C$. As θ approaches this limit, v becomes infinite, and the trajectory becomes a straight line. The angle β can be used as the trajectory parameter instead of C. Actually, of course, the angle of elevation can never approach β closely, for the square law will cease to apply long before that.

Having the hodograph equation, we now come to the computation of the trajectory, i.e., of the coordinates x, y of the shell[1]. This requires additional quadrature, this time not with θ alone, but with C as a parameter.

The element of the horizontal displacement of the shell is $dx = v\cos\theta\, dt$; but from (1) $dt = -v\, d\theta/g\cos\theta$, and therefore $dx = -v^2 d\theta/g$; substituting the expression for v^2 from (6), we have $dx = -d\theta/2cc\cos^2\theta(C - \xi)$. Clearly, an expression like 2cdx would be more general (for it would not depend upon c, but only upon θ and C):

$$2cdx = -\sec^2\theta\, d\theta/(C - \xi) \qquad (7)$$

[1] Consistent units are assumed.

The element of the vertical displacement of the shell is $dy = \tan\theta\, dx$, and therefore

$$2cdy = -\sec^2\theta \tan\theta\, d\theta/(C - \xi) \tag{8}$$

Incidentally, the element ds of the arc of the trajectory is directly integrable:

$$2cds = \sqrt{(2cdx)^2 + (2cdy)^2} = \sec^2\theta\sqrt{1 + \tan^2\theta}\, d\theta/(C - \xi) = d\xi/(C - \xi) = d\ln(C - \xi) \tag{9}$$

To get the time of flight, we substitute (6) into (1):

$$dt = -v\, d\theta/g\cos\theta = -(\sec\theta\sqrt{g/2c(C - \xi)})\, d\theta/g\cos\theta,$$

or more generally,

$$\sqrt{2gc}\, dt = -\sec^2\theta\, d\theta/\sqrt{C - \xi} \tag{10}$$

All of these quantities can be integrated between any desired values of θ. We are primarily interested in the terminal data, i.e., range X_c, time of flight T and possibly, the arc S; generally $Y = 0$. To get X_c, T and S we have to integrate from $\theta = \phi$, the angle of elevation, to $\theta = -\omega$, where ω is the angle of fall, reckoned positive as is customary. Here we see that these quadratures turn out to be rather cumbersome; for not only do we lack the explicit forms of these integrals (except for S), but in order to estimate any one of them, say X_c, we need an exact value of ω. To get this we have to integrate 2cdy (which we otherwise may not need) from ϕ thru the summit till $y = Y = 0$ again; the resultant ω will be determined by the interpolation for $y = 0$ from a set of tabulated values of $y(\theta)$.

In order to make the use of the square law of drag practicable, it is therefore necessary to make all the integrations and interpolations beforehand, once and for all, so that any particular problem could be solved by a simple interpolation. The construction of such numerical data (viz., of the Otto-Lardillon tables and of various ways of plotting them) is discussed in Appendix II.

A brief table of $\xi(\theta) = \int_{\theta}^{0} \sec^3\theta d\theta$*

θ	$\xi(\theta)$	θ	$\xi(\theta)$	θ	$\xi(\theta)$
0°	0.00000	30°	0.608	60°	2.391
1	0.01746	31	0.635	61	2.537
2	0.03493	32	0.663	62	2.698
3	0.0524	33	0.693	63	2.875
4	0.0700	34	0.723	64	3.072
5	0.0876	35	0.754	65	3.290
6	0.1053	36	0.786	66	3.535
7	0.1231	37	0.820	67	3.811
8	0.1410	38	0.855	68	4.123
9	0.1590	39	0.891	69	4.477
10	0.1772	40	0.929	70	4.884
11	0.1956	41	0.969	71	5.354
12	0.2141	42	1.010	72	5.901
13	0.2329	43	1.054	73	6.544
14	0.2519	44	1.100	74	7.307
15	0.2711	45	1.148	75	8.224
16	0.2906	46	1.198	76	9.338
17	0.3104	47	1.252	77	10.71
18	0.3305	48	1.309	78	12.44
19	0.3510	49	1.369	79	14.65
20	0.3719	50	1.432	80	17.55
21	0.3931	51	1.500	81	21.45
22	0.415	52	1.573	82	26.89
23	0.437	53	1.650	83	34.81
24	0.460	54	1.733	84	46.99
25	0.483	55	1.822	85	67.14
26	0.506	56	1.918	86	104.18
27	0.531	57	2.022	87	184.12
28	0.556	58	2.135		
29	0.582	59	2.257		

*For a more extensive table, see Cranz; also extensive tables of $\sin\theta(\xi)$ and $\cos\theta(\xi)$ have been prepared.

APPENDIX II

CONSTRUCTION OF THE OTTO-LARDILLON TABLES AND CHARTS

The computation of the trajectory, and particularly of the terminal data (mainly X and T) of the trajectory based on the square law of drag, was given in Appendix I. It can be summarized as follows:

Given $c = K_D \rho d^2/m$ (a constant characterizing the shell), the muzzle velocity V and the angle of departure ϕ, we

(1) introduce an auxillary tabulated variable $\xi(\theta) = \int_0^\theta \sec^3\theta d\theta$;

(2) compute the trajectory parameter C, defined by the hodograph equation as

$$C = \xi(\phi) + g/2cV^2\cos^2\phi;$$

(3) compute the altitude of the summit y_s by performing the quadrature

$$2cy_s = -\int_\phi^\theta \sec^2\theta\tan\theta d\theta/(C - \xi);$$

(4) continue this integration with the negative values of θ (and ξ) and evaluate this integral from $\theta = 0$ to several negative values of θ such that the values of the integral, taken from $\theta = \phi$, would bracket zero sufficiently closely;

(5) interpolate between these values of 2cy for $y = Y = 0$, obtaining $\theta = -\omega$, ω being the angle of fall; and finally,

(6) compute the range X_c from

$$2cX_c = -\int_0^\omega \sec^2\theta d\theta/(C - \xi),$$

(7) compute the time of flight T from

$$\sqrt{2gc}\, T = -\int_0^\omega \sec^2\theta d\theta/\sqrt{C - \xi} \quad \text{(this is } = \gamma\sqrt{2})$$

(8) and, if desired, compute the length S of the trajectory from

$$2cS = \ln\frac{C - \xi(-\omega)}{C - \xi(\phi)}$$

It is clear that in performing the quadratures for y, x, t and s it is a simple matter to mark the values of all these integrals for several intermediate round values of θ on the ascending branch of the

trajectory. Similarly, once the values of y(θ) on the descending branch are tabulated sufficiently closely, it is a relatively simple matter to interpolate for such negative values of θ that the altitudes of the shell, the y's, would equal those for which the round values of θ occurred on the ascending branch. We shall then have, as parts of our sought trajectory, a series of horizontally sliced segments. Each of these component trajectories represents a trajectory of its own, with the same C, but with different ϕ's and (it will be noted from the hodograph equation) with different V's. Similarly, we can consider our trajectory as a segment of a larger one that starts with a greater ϕ and V. To obtain this larger trajectory, we can extend these integrals separately on the ascending and the descending branch, as long as ϕ does not approach its limit β, defined by $C = \xi(\beta)$, too closely. By performing this calculation for a series of values of C one can cover the whole domain of the possible and practicable trajectories in the dimensionless coordinates 2cX, 2cY, and $T\sqrt{2gc}$, each of these generalized trajectories being applicable to all practicable values of c.

While Cranz gives the Otto-Lardillon tables without a detailed explanation of how they were constructed from the above-listed integrals, one need not doubt that the procedure had been essentially as described here; except that the integrals were subsequently interpolated so as to eliminate the parameter C, and so that the integrals would be tabulated against $2cX_c$. A sample of these tables is given below. As for the notation, ours differs from Cranz's only in the use of X_c for X (we reserve X for the range in the non-consistent units of yards) and in the use of capital V's for the terminal velocities (V for v_o and V_e for v_e). The tables are given for $\phi = 1°, 5°, 10°, 15°, \ldots\ldots 75°$.

$2cX_c$ ($=\nu$)	cV^2/g ($=\eta^2$)	$V^2/2gX_c$ ($=1/\mu$)	ω	V_e/V	$T\sqrt{g/X_c}$	y_s/X_c
0.000	0.000	0.577	60°00′	1.000	1.861	0.433
0.05	0.029	0.592	60°32′	0.981	1.870	0.437
0.10	0.060	0.608	61°03′	0.962	1.880	0.442
....	....	....	....	....	....	....
1.45	2.040	1.407	73°33′	0.543	2.169	0.593

It might well be demonstrated that all quantities listed in the Otto-Lardillon tables are determined directly from the integrals listed above.

a. The first column, $2cX_c$, is directly one of these integrals; it is used as the auxiliary variable ν in our charts.

b. The ratio of the maximum drag to the acceleration of gravity, cV^2/g, is determined by C and ϕ from the hodograph equation written as

$$cV^2/g = 1/2\cos^2\phi(C - \xi(\phi))$$

c. The ratio $V^2/2gX_c$ is simply $(cV^2/g)/(2cX_c)$; the reciprocal of this ratio, μ, is used as the abscissa of our charts.

d. The angle of fall, ω, is fixed for any trajectory that can be defined by any three data (say, c, V and ϕ) from c, V, ϕ, η, μ, ν, C, etc.

e. The ratio of the striking velocity to the muzzle velocity, V_e/V, is completely determined by C and ϕ, as can be seen from the hodograph equation, written once for the muzzle conditions as in (b) above, and once again for the instant of fall:

$$cV_e^2/g = 1/2\cos^2(-\omega)\,(C - \xi(-\omega)),$$

and taking the ratio.

f. The dimensionless variable in terms of which the time of flight is given, $T\sqrt{g/X_c}$, is simply $(T\sqrt{2gc})/(\sqrt{2cX_c})$.

g. The ratio y_s/X_c is simply $2cy_s/\nu$.

Cranz also gives plots of these tables, viz., the plots of cV^2/g, $V^2/2gX_c$, $T\sqrt{g/X_c}$, $\omega - \phi$, V_e/V and y_s/X_c, versus $2cX_c$ for various ϕ's. The latter three plots are reproduced in Fig. 5 of this report. The first three would suffice for most of the usual mortar fire problems, except that their scale is small. However, it appeared preferable to combine these first three plots on one chart, largely because it is more convenient to use one chart instead of three[1].

One such plot, of η versus $\zeta = \sqrt{V^2/2gX_c} = 1/\sqrt{\mu}$, with a nomogram for $T\sqrt{g/X_c}$, has been given in BRLM 434. It appeared desirable, however, to have a larger plot, with a better means of handling T, with the data on ν, and one that would extend to $\phi = 90°$; for this purpose the present charts were made. The details of construction of the charts will be obvious after a study of the Otto-Lardillon tables. A word might be added as to the selection of variables for plotting. The quantity η, rather than η^2, has been selected mainly for the purpose of shrinking the upper regions on the chart, and stretching the lower regions; also it is convenient to have the ordinate proportional to V, rather than to V^2. The quantity μ has been selected because it reflects the variation of X most vividly, and also because it permitted stretching the chart near $\phi = 45°$ and shrinking near $\phi = 0°$ or 90°. The lines of ν (straight in the η vs. ζ plot) are easy to compute without reference to the Otto-Lardillon data, for $\eta^2\mu = 1$. The time variable $\gamma = T\sqrt{gc}$ (note that this is the time integral (10), but without the factor $\sqrt{2}$) was selected for several reasons discussed in the body of this report, but mainly because it allowed the extension of the charts to $\phi = 90°$; for $T\sqrt{g/X_c}$ then becomes infinite and other (otherwise convenient) dimensionless variables containing T^2 are difficult to estimate at $\phi = 90°$.

The square-law formulas for a vertical trajectory might be cited as a matter of general interest:

a. For the ascending branch, if velocity v is positive upwards and $dv = (-g - cv^2)dt$;
$T_a = (\tan^{-1}\eta)/\sqrt{gc}$; $y_{max} = (1/2c)\ln(1+\eta^2)$.

b. For the descending branch, if v is positive downward, $dv = (g - cv^2)dt$, and $\eta_e = V_e/\sqrt{g/c}$, where V_e is the striking velocity: $T_d = (1/2\sqrt{gc})\ln\left((1+\eta_e)/(1-\eta_e)\right)$; $y_{max} = -(1/2c)\ln(1-\eta_e^2)$;

[1] There were a few other practical reasons. Consider, for instance, a typical problem: to find the drag, or c, from the firing data ϕ, V, X. Now, ϕ and V are usually accurately known and do not vary much, while the variation of X is large. We have to enter the tables, or charts, with some $\mu = \mu(V,X)$ and ϕ; but we would prefer the result (containing c) to be independent of the uncertain X, i.e., we would prefer $\eta(c,V)$ to $\nu(c,X)$.

[2] One quantity considered was $T\sqrt{g/X_c}\tan\phi$ (or, mnemonically, $T/\sqrt{(V\sin\phi/g)(X_c/V\cos\phi)}$) which varies in very narrow limits.

c. hence, the total time of flight

$$T = (2\tan^{-1}\eta + \ln((1 + \eta_e)/(1 - \eta_e))/2\sqrt{gc}, \text{ where } 1 + \eta^2 = 1/(1 - \eta_e^2), \text{ or}$$

$$\eta_e = \eta/\sqrt{1 + \eta^2}.$$

It might be interesting to cite the proof that the lines of constant ϕ are perpendicular to the bottom line on the chart, i.e., that $\lim(\partial\mu/\partial\eta)_\phi$, as η approaches 0, is zero. Here $\mu = 2gX/V^2$ and $\eta = V\sqrt{c/g}$; only c and X vary. Then $d\eta = (V/2\sqrt{gc})dc$, and $d\mu/d\eta = (2g/V^2)dX/(V/2\sqrt{gc})dc = (4g\sqrt{gc}/V^3)dX/dc$. Since for any arbitrarily small finite c, in the nature of the problem, dX/dc cannot be infinite, this expression vanishes with $\sqrt{c}$.

For eventual application of the adjoint method of correction for mortar fire, and particularly, for estimating the effect of stability and yawing motion of the shell, as per McShanes's BRL Reports Nos. 327 and 337, as well as for some other occasions, the construction of a particular trajectory will often be desired. With the Otto-Lardillon tables we can find the C of that trajectory and the altitude of the summit; then we can determine the terminal data for a trajectory which constitutes a segment of ours, and which occurs above such an altitude that the inclination θ on the ascending branch of our trajectory has a round value. For the new component trajectory we have the same C, a new η, which is determined by the new ϕ (the round value of θ) from the hodograph equation, and a new altitude of summit. We can easily place the two trajectories so that their summits are at the same level; however, in order to make them coincide both in X and T, we need the summital values of the X and T integrals, which are lacking in the Otto-Lardillon tables. These have been computed for a few C's (for that work is relatively simple, as it does not involve computation of the 2cy integral, nor the interpolation). The results are given in Tables I and II and plotted in Fig. 3. A sample of the construction of a trajectory is given in Appendix IV.

The extension of the Otto-Lardillon tables from 75° to 85°, made as indicated in Appendix I to BRLM 434, is not a very reliable process; for a point on the 75° curve, when considered as a section of the 85° trajectory with the same trajectory parameter C, corresponds to a much higher η. Thus only a few points on the 85° curve could be obtained, and the errors of the Otto-Lardillon tables that were quite tolerable for small η's must have been necessarily exaggerated. For these reasons much attention was given to the various methods of graphical interpolation, and to the computation of the limiting case $\phi = 90°$, which allowed drawing the ϕ and γ lines through the difficult region by interpolation.

TABLE I

Extension of the Otto-Lardillon tables to larger ϕ's
(point marked by black circles on large chart.)

ν at 75°	C	ϕ	$V\sqrt{c/g} = \eta$	Δ(2cy)	ω	V_e/V_o	$2cX_c = \nu$	Y_s/X_c	$2gX_c/V^2 = \mu$	$\sqrt{2gc}T = \gamma$
.05	151.696	80°	.352	.06569	80°37'	.942	.0773	1.463	.625	.9527
		85°	.882	.5306	86°23'	.761	.1759	9.4457	.226	2.172
.10	76.670	80°	.530	.1432	81°15'	.881	.1513	1.516	.563	1.385
		85°	2.628	2.3958	88°42'	.366	.4894	9.5821	.0709	3.890
.15	52.122	80°	.693	.2335	81°54'	.818	.2417	1.573	.504	1.746
.20	39.849	80°	.862	.3417	82°34'	.753	.3302	1.636	.444	2.082
.25	32.373	80°	1.058	.4774	83°17'	.683	.4261	1.712	.381	2.424
.30	27.407	80°	1.297	.6515	84°05'	.608	.5325	1.800	.317	2.779
.35	23.869	80°	1.620	.8878	84°55'	.513	.6524	1.919	.248	3.177
.40	21.248	80°	2.117	1.2362	85°54'		.7993	2.077	.178	3.674
at 80° (interpolated)	C	ϕ	$V\sqrt{c/g} = \eta$	Δ(2cy)	ω	V_e/V_o	$2cX_c = \nu$	Y_s/X_c	$2gX_c/V^2 = \mu$	$\sqrt{2gc}T = \gamma$
.010	1130.5	85°	.249	.0454	85°08'	.967	.0204	2.920	.330	.6878
.025	458.6	85°	.410	.1184	85°22'	.922	.0518	2.981	.308	1.119

TABLE II

Computation of Summital Data

θ	C	$V\sqrt{c/g}$ $-\eta$	$2cX_s$ $-\nu_s$	$T\sqrt{gc}$ γ_s	C	$V\sqrt{c/g}$ $-\eta$	$2cX_s$ $-\nu_s$	$T\sqrt{gc}$ $-\gamma_s$	C	$V\sqrt{c/g}$ $-\eta$	$2cX_s$ $-\nu_s$	$T\sqrt{gc}$ $-\gamma_s$	C	$V\sqrt{c/g}$ $-\eta$	$2cX_s$ $-\nu_s$	$T\sqrt{gc}$ $-\gamma_s$
0	120	.0645	0	0	10	.224	0	0	3	.408	0	0	1	.707	0	0
5		.0648	.00073	.0057		.225	.00880	.0196		.416	.0296	.0360		.743	.0918	.0634
10		.0656	.00147	.0114		.229	.0178	.0396		.427	.0606	.0731		.792	.194	.131
15		.0669	.00224	.0173		.235	.0272	.0603		.443	.0936	.112		.857	.312	.204
20		.0688	.00304	.0235		.243	.0371	.0822		.464	.129	.153		.949	.454	.287
25		.0714	.00389	.0301		.253	.0478	.106		.492	.169	.199		1.085	.633	.383
30		.0747	.00482	.0375		.266	.0595	.131		.528	.215	.249		1.304	.879	.499
35		.0791	.00585	.0454		.284	.0728	.160		.576	.267	.306		1.740	1.272	.655
40		.0846	.00702	.0544		.306	.0879	.192		.641	.332	.373		3.468	2.382	.920
45		.0917	.00837	.0649		.336	.106	.230		.735	.414	.454		—		
50		.1010	.00999	.0773		.376	.128	.276		.879	.526	.557		—		
55		.1134	.0120	.0927		.431	.156	.334		1.136	.700	.701				
60		.1304	.0146	.113		.513	.197	.410		1.812	1.062	.933				
65		.1549	.0181	.140		.646	.252	.520		—						
70		.1927	.0233	.179		.914	.356	.696		—						
75		.2584	.0321	.245		2.050	.696	1.116		—						
80		.4023	.0504	.379						—						
85		1.002	.1437	.916						—						
0	20	.158	0	0	5	.316	0	0	2	.500	0	0				
5		.159	.00439	.0139		.320	.0176	.0278		.513	.0448	.0452				
10		.161	.00886	.0279		.327	.0359	.0563		.532	.0923	.0916				
15		.165	.0135	.0433		.337	.0551	.0859		.557	.144	.140				
20		.170	.0184	.0578		.350	.0756	.117		.590	.201	.193				
25		.177	.0236	.0742		.367	.0980	.151		.633	.266	.250				
30		.185	.0293	.0920		.390	.123	.188		.692	.343	.316				
35		.197	.0357	.1117		.419	.151	.230		.773	.436	.391				
40		.211	.0429	.1342		.457	.185	.278		.892	.556	.482				
45		.230	.0514	.1603		.510	.225	.336		1.083	.725	.599				
50		.255	.0617	.1917		.582	.277	.406		1.460	.999	.761				
55		.289	.0746	.2307		.692	.347	.497		2.923	1.786	1.061				
60		.337	.0915	.2815		.875	.453	.624		—						
65		.409	.116	.3520		1.280	.649	.825		—						
70		.532	.154	.4590		6.077	3.03	1.541								
75		.794	.229	.6520		—										
80		2.600	.357	1.298		—										
85		—				—										

APPENDIX III

DERIVATION OF DIFFERENTIAL CORRECTIONS

Having obtained graphically the dimensionless derivatives discussed under "Differential Corrections," pp. 9 - 10, viz.,

$$k_1 = \left|(\partial\mu/\partial\eta)_\phi\right| \qquad k_3 = (\partial\gamma/\partial\eta)_\phi$$

$$k_2 = \left|(\partial\mu/\partial\phi)_\eta\right| \qquad k_4 = (\partial\gamma/\partial\phi)_\eta \ ,$$

we can evaluate the differential corrections as follows:[1]

$\partial X/\partial V$:

$$-k_1 = (\partial\mu/\partial\eta)_\phi = d(2gX_c/V^2)/d(V\sqrt{c/g})$$

$$= \left[(2g/V^2)dX_c - 2(2gX_c/V^3)dV\right] / \left[(\sqrt{c/g})dV\right]$$

$$= \left[(\mu V/X_c)\, dX_c/dV - 2\mu\right]/\eta$$

$$\therefore\ \partial X/\partial V = (X/V)(2 - k_1\eta/\mu)$$

$\partial X/\partial\phi$:

$$-k_2 = (\partial\mu/\partial\phi)_\eta = d(2gX_c/V^2)/d\phi$$

$$= (2g/V^2)dX_c/d\phi$$

$$= (\mu/X_c)dX_c/d\phi$$

$$\therefore\ \partial X/\partial\phi = -Xk_2/\mu$$

$\partial X/\partial C_s$:

(a) $$-k_1 = d(2gX_c/V^2)/(V\sqrt{c/g})$$

$$= (2g/V^2)dX_c/(-.5V/\sqrt{gc})dc$$

$$= (\mu/X_c)dX_c/(-.5\,\eta/c)dc$$

$$= -(2\mu c/X_c\eta)dX_c/dc$$

$$\therefore\ \partial X/\partial c = (X/c)(k_1\eta/2\mu)$$

---

[1] In deriving formulas containing the range in common units (X), we omit an intermediate step, viz., the formulas containing the range in consistent units (X_c); for the formulas, being dimensionally consistent, are usually the same in either set of units.

(b) $c = 1/19174C_s$

$$dc = -(1/19174C_s^2)dC_s = -(c/C_s)dC_s$$

$$1/dc = -(C_s/c)/dC_s$$

$$-(C_s/c)dX/dC_s = (X/c)(k_1\eta/2\mu)$$

$$\therefore \partial X/\partial C_s = -(X/C_s)(k_1\eta/2\mu)$$

$\partial T/\partial V$:

$$k_3 = (\partial\gamma/\partial\eta)_\phi = d(T\sqrt{gc})/d(V\sqrt{c/g})$$

$$= (\sqrt{gc})dT/(\sqrt{c/g})dV$$

$$= g\ dT/dV$$

$$\therefore \partial T/\partial V = k_3/g$$

$\partial T/\partial\phi$:

$$k_4 = (\partial\gamma/\partial\phi)_\eta = d(T\sqrt{gc})/d\phi$$

$$= (\sqrt{gc})dT/d\phi = (\gamma/T)dT/d\phi$$

$$\therefore \partial T/\partial\phi = k_4 T/\gamma$$

$\partial T/\partial C_s$:

(a) $$k_4 = (\partial\gamma/\partial\eta)_\phi = d(T\sqrt{gc})/(V\sqrt{c/g})$$

$$= \left[\sqrt{gc}\ dT - .5T\sqrt{g/c}\ dc\right] / \left[.5(V/\sqrt{gc})dc\right]$$

$$= \left[(2\gamma c/T)dT/dc - \gamma\right]/\eta$$

$$\therefore \partial T/\partial c = (T/2\gamma c)(k_4\eta - \gamma)$$

(b) $$\therefore \partial T/\partial C_s = (T/2C_s)(1 - k_4\eta/\gamma)$$

In deriving the corrections for wind, we consider for the present time only the usual ballistic corrections; i.e., we consider the shell fired in a system of coordinates moving with the wind (so that the vector of the muzzle velocity in that system of coordinates, when added to the vector of the wind velocity, equals the vector of the muzzle velocity with respect to the ground). Also, we consider only the case when the wind velocity W is small in comparison with both horizontal and vertical components of muzzle velocity V. Furthermore, since the axis of the shell at the commencement of the trajectory is along the actual ve-

locity vector (V), in the moving system of coordinates the shell starts its trajectory with a certain yaw; this fact is neglected.

We denote the terminal data of the actual trajectory (with wind) by ϕ, V, X, Z and T, while the terminal data for the (windless) trajectory in the moving coordinates are denoted by ϕ', V', X', Z' and T'. For simplicity we express the wind velocity W in fps. Then the change in V, ϕ and the azimuth of fire is given by the equations (See sketch)

$$V' - V = dV = - W_x \cos\phi$$

$$\phi' - \phi = d\phi = (W_x \sin\phi)/V$$

$$\text{(change in azimuth of V)} = - W_z/V\cos\phi$$

The corrections for a small cross-wind W_z are well known:

$$\partial X/\partial W_z = 0$$

$$\partial T/\partial W_z = 0$$

$$\partial Z_c/\partial W_z = T - X_c/\cos\phi^1 \text{ ft/fps, or}$$

$$\partial Z/\partial W_z = T/3 - X/V\cos\phi \text{ yds/fps}$$

The corrections for the small range wind W_x are:

$$(\partial X_c/\partial W_x)\, W_x = X_c' + T'W_x - X_c$$

$$\partial X_c/\partial W_x = T' + (X_c' - X_c)/W_x$$

$$= T' + \left((\partial X_c/\partial\phi)d\phi + (\partial X_c/\partial V)dV \right)/W_x$$

$$= T + dT + (-X_c k_2/\mu)(\sin\phi/V) + (X_c V)(2 - k_1\eta/\mu)(-\cos\phi)$$

$$= T - (X_c/V)(2\cos\phi - k_1\eta\cos\phi/\mu + k_2\sin\phi/\mu) + dT$$

or, neglecting the second-order term,

$$\partial X/\partial W_x = T/3 - (X/V)\left[2\cos\phi - (k_1\eta\cos\phi - k_2\sin\phi)/\mu \right].$$

Also,

$$(\partial T/\partial W_x)W_x = T' - T = (\partial T/\partial\phi)d\phi + (\partial T/\partial V)dV$$

$$\partial T/\partial W_x = (k_4 T/\gamma)(\sin\phi/V) + k_3/g)(-\cos\phi)$$

and, of course,

$$\partial Z/\partial W_x = 0.$$

$$\overline{I_{dZ_c} = Z_c - Z_c'} = Z_c = (\partial Z_c/\partial W_z)W_z = W_z T + X_c(-W_z/V\cos\phi).$$

APPENDIX IV

EXAMPLES OF THE USES OF THE CHARTS

To illustrate the use of the chart, let us consider the results of firing 10 rounds of the standard 105 mm mortar shell T17E1 at the Trench Warfare Range, APG, on 28 June 1946 (Firing Record P40860). While the purpose of these firings was the analysis of dispersion, in the present instance we shall limit ourselves to treating the average data and to working out the differential corrections that might be later applied to the individual ranges.

Consider first the following average data:

$\phi = 68°$

V = 747 fps

X = 2792 yds.

T = 39.4 sec.

These data are not corrected for wind; since we do not have the corrections for winds as yet, we neglect these corrections for the time being. We compute $\mu = 193(2792)/747^2 = .966$, locate a point on the 68° line (Fig. 1) and read $\eta = .754$, $\gamma = 1.243$. Therefore,

$$C_{sx} = (747/[785 \times .754])^2 = 1.592$$

$$C_{st} = (39.4/[24.4 \times 1.243])^2 = 1.688$$

The X, T discrepancy, or $C_{st}/C_{sx} - 1$, is 6.0%. The fact that this discrepancy is positive (or that the ballistic coefficient for the time of flight is greater than the ballistic coefficient for the range) indicates the presence of either lift effect, or adverse wind, or both (i.e., the shell could have kited and stayed in the air longer, but without a corresponding gain in range; or the adverse wind has shortened the range without a corresponding reduction in time of flight).

To get the differential corrections for wind, we obtain by graphical differentiation (from Fig. 1):

$k_1 = -(\partial\mu/\partial\eta)_\phi = .76$ $\qquad$ $k_2 = -(\partial\mu/\partial\phi)_\eta = .0345$

$k_3 = (\partial\gamma/\partial\eta)_\phi = 1.31$ $\qquad$ $k_4 = (\partial\gamma/\partial\phi)_\eta = .0090$

Hence,

$$\partial X/\partial W_x = 39.4/3 - (2792/747)\left[2 \times .3746 - (.76 \times .754 \times .3746 - .0345 \times .9272)/.966\right]$$

$$= 13.13 - 3.74\,(.7492 - .2146 + .0320) = 11.01 \text{ yds/fps, or } .394\% \text{ of X, and}$$

$$\partial T/\partial W_x = (.0090 \times 39.4/747)\ .9272 - (1.31/32.2)\ .3746$$

$$= .00044 - .01524 = -.0148 \text{ sec/fps, or only } -.038\% \text{ of T}$$

(cf. par. a. on page 8); also, of course,

$$\partial Z/\partial W_z = 13.13 - 3.74/.3746 = 3.15 \text{ yds/fps.}$$

Observing $\nu = 2cX_c = .55$, we find, from Fig. 5, $y_{max}/X = .760$; hence the maximum ordinate = .760 x 2792 = 2122 yards. Now we cut off the available meteorological data at this altitude, and get the effective ballistic winds. In this case, the weighted range wind is approximately -13.2 mph; the average wind, -12.2 mph, differs little from the weighted one. The cross-wind is small, averaging + 1.5 mph; the correction for it, 1.5(1.467)3.15 = + 7 yds.[1], agrees well with the average value of observed deflection, +3 yards, but is rather meaningless in comparison with the large dispersion (maximum dispersion 105 yds.). The effect of the range wind on the time of flight is -13.2(1.467)(-.0148) = + .287 seconds. The correction of the range is -13.2(1.467)(11.01) = -213 yards; this is quite noticeable even when compared with the dispersion (std. dev. 147 yds.)

The range corrected for the range wind turns out to be 2792 - (-213) = 3005 yards; the new time of flight is 39.4 - (+.28) = 39.1 sec.; the new μ is .966(3005/2792) = 1.040; the new η = .658 and the new γ = 1.115. Hence new C_{sx} = 2.091, and the new C_{st} = 2.093. The discrepancy has thus practically vanished, indicating that the lift effect is not noticeable within the accuracy of this experiment.

For the new point we obtain,

$k_1 = .70$ $\qquad$ $k_2 = .0367$

$k_3 = 1.412$ $\qquad$ $k_4 = .0079$

(it might be noted that too much stock should not be placed in the variation of these derivatives from point to point). Now the differential corrections can be computed as follows:

$$\partial X/\partial V = (3005/747)(2 - .70 \times .658/1.040) = 4.02(2 - .443) = 6.26 \text{ yds/fps.}$$

$$\partial X/\partial \phi = -3005 \times .0367/1.040 = -106 \text{ yds/degree;}$$

$$\partial X/\partial C_{sx} = (3005/2.091)(.443/2) = 666/2.091 = 319 \text{ yards per unity of ballistic coefficient,}$$

or 6.66 yards per 1% of C_{sx};

$$\partial X/\partial W_x = 39.1/3 - 4.02\left[.7492 - (.461 \times .3746 - .0367 \times .9272/1.040) \right] =$$

$$= 10.58 \text{ yards/fps (not in bad agreement with the previous figure 11.01 yds/fps);}$$

$$\partial T/\partial W_x = (.0079 \times 39.1/747)\ .9272 - .0439 \times .3746$$

$$= .000383 - .01644 = -.0161 \text{ sec/fps;}$$

$$\partial T/\partial V = 1.412/32.2 = .0439 \text{ sec/fps;}$$

$$\partial T/\partial \phi = .0079 \times 39.1/1.115 = .277 \text{ sec/degree;}$$

[1] 1 mph = (5280/3600) fps = 1.467 fps.

$\partial T/\partial C_{st}$ = (39.1/2 x 2.093)(1 - 1.412 x .662/1.119) =

= (19.55/2.093)(1 - .835) = 3.23/2.093 = 1.54 seconds per unity of C_{st} or .0323 seconds per 1% of C_{st}

$\partial Z/\partial W_z$ = 13.03 - 4.02/.3746 = 2.30 yds/fps.

To give an example of the use of the ν-lines, suppose it is desired to determine the muzzle velocity of 4.2 in. chemical mortar HE shell M3, necessary in order to give, at ϕ = 50° = 889 mils, a range of 1670 yards; and that the calculations should be based on the data from FT 4.2-B-1, and specifically, on a point (X = 2850, ϕ = 1030 mils = 57.9°, 16 rings or V = 649 fps) that is fairly remote from the desired point. We compute $\mu = 193(2850/649^2) = 1.036$, and for ϕ = 57.9° read η=.695. Hence, $\nu = .695^2 \times 1.036 = .6308$; the new ν is .6308(1670/2850) = .370; for ϕ = 50° and this ν we read η = .467; the desired velocity is 649(.467/.695) = 436 fps. It is interesting to compare this value with that interpolated from the firing table; at 889 mils, with 8 rings (V = 428), X = 1603, and with 9 rings (V = 459), X = 1807; for X = 1670 the desired velocity comes out 438 fps.

As still another example (this time with fictitious figures) suppose that a mortar-type projectile was fired at a demonstration, where the means for the measurement of velocity were not available, and that the only available data are ϕ = 55°, X = 1293, T = 20.9; it is desired to find the approximate values of V and C_s. Now the relevant variable is $T\sqrt{g/X_c}$ = say f, which has not been plotted, as it is seldom wanted (cf. par. "b" and "d" on page 9); we have to find the point $f = 20.9\sqrt{32.2/(1293 \times 3)} = 1.904$ on the line ϕ = 55°. Since $f = \sqrt{2}\,(T\sqrt{gc})/\sqrt{2cX_c} = \gamma\sqrt{2}/\eta\sqrt{\mu}$, we get for a few points on this line:

γ =	1.6	1.5	1.4
η =	1.225	1.125	1.021
μ =	.905	.979	1.061
f =	2.040	1.928	1.827

Interpolating, γ = 1.428. Since this is $20.9/24.4\sqrt{C_s}$, $\sqrt{C_s}$ = (20.9/24.4)/1.482 = .578; C_s = .335. To get V, we read either η = 1.107 = V/(785 x .578), whence V = 1.107 x 785 x .578 = 502 or μ = .992 = $193(1293)V^2$, whence $V = \sqrt{193(1293)/.992} = 501$.

Finally, suppose it is desired to construct the trajectory characterized by ϕ = 50.5°, μ = 1.168. Then η = .966, $\nu = \eta^2\mu = 1.168 \times .966^2 = 1.090$; from Fig. 4, y_s/X = .375 and hence $2cy_s = (y_s/X)(2cX)$ = .375 x 1.090 = .409; from Fig. 3 for this η and ϕ, μ_s = .635 and hence $\nu_s = \eta^2\mu_s = .966^2 \times .635 = .592$; from Fig. 5 $\omega - \phi$ = 11.4° or ω = 61.9°. The parameter for this trajectory is $C = \xi(50.5°) + 1/2 \times \eta^2 \times \cos^2 50.5° = 1.465 + 1/2 \times .966^2 \times .636^2 = 2.791$. Now, let θ = 45°; then $\eta^2 = 1/2 \cos^2\theta\,(C - \xi(\theta))$ = $1/2(.707)^2\,(2.791 - 1.148) = .609$; η = .780; μ (from Fig. 1) = 1.389, ν = .845, y_x/X = .292; $2cy_s = .846 \times .292 = .247$, or the 45° trajectory starts at an altitude y defined by 2cy = .409 - .247 = .162; also $\omega - \theta$ = 8.88° or the inclination of the descending branch at that altitude is 53.88°. We need perhaps only two additional levels, characterized say by θ = 30° and 20°, to plot this trajectory sufficiently close. For a certain η_θ and μ, values of γ can be determined by interpolation from Figs. 1 and 2. The values of γ_s are determined, by interpolation, for a given constant C (viz. 2.791) from Fig. 4. The results are plotted to scale in Fig. 6.

APPENDIX V

COMPARISON OF THE SQUARE LAW WITH THE GAVRE FUNCTION FOR TYPICAL MORTAR SHELL

Ideally, a mortar shell should be characterized by a single value of ballistic coefficient; this value should hold for all muzzle velocities and all elevations. To fit the actual performance of the shell, however, it is necessary to vary the ballistic coefficient as the muzzle velocity and the elevation vary. It is natural to presume that such variation of ballistic coefficient is due to the fact that the drag function used is not the right one for the shell in question[1]. Accordingly, a drag function may be considered to represent a shell better, the smaller the variation in ballistic coefficient.

A comparison of the square law with the Gavre function is given in the following tabulation. The ballistic coefficients of several mortar shell were computed in two ways, viz., by the use of the Gavre function (values of C_1) and by the square law (values of C_s). The values of C_1 are the ones computed in the preparation of the firing tables for these shell; they are based on range firings, all practicable corrections for the meteorological conditions (and, presumably, some smoothening) having been applied. The values of C_s were computed with the square-law charts on the basis of range and velocity data contained in these firing tables.

The comparison of the absolute values of C_1 and C_s would be rather meaningless, for the assumed standard square-law function ($K_D = 0.1$) is not intended to represent the Gavre shell. One can compare only the relative variation of C_1 and C_s with the muzzle velocities and with the elevations.

In judging which function represents the shell better, one should be cautious, for the ballistic coefficients determined from the range data are not too reliable, particularly at lower muzzle velocities (since the change in range produced by a change in the drag function or in the ballistic coefficient may be completely masked by the present-day dispersion of mortar shell).

It might be mentioned that the smoothening of the range data might have been done with an intention to reduce the variation in C_1; while the shown values of C_s were not subjected to any smoothening.

It might also be mentioned that in those cases where C_s varies with the maximum altitude, this variation may be ascribed not the variation of K_D, but to a variation of an "average" air density, ρ; for in the square-law theory it is only necessary to assume a constant product $K_D\rho$ (see par. 2 on page 6).

From an inspection of this tabulation it will be seen that the square law represents the present-day mortar shell as well as the Gavre function and perhaps better. Thus, the a priori expectation that the drag coefficient of mortar shell is more nearly constant than the drag coefficient of the Gavre function (see page 5, paragraph "thirdly") is confirmed.

---

[1] The deviation from the "particle trajectory" being assumed to be secondary.

COMPARISON OF C_1 AND C_s

Values of C's

	Muzzle Velocity (fps)	C_1 (assumed the same for all elevations)	C_s (average for all elevations, given in the F.T.)	Variations of C's with elevation. C_1 (maximum variation % of average value)	C_s
60mm Mortar Shell M49A2 (FT 60-A-2)					
	225	.798	.788	-	30.2
	313	.714	.765	-	37.3
	387	.676	.745	-	14.8
	458	.657	.751	-	13.7
	518	.650	.757	-	17.3
Maximum variation % of average value		21.2	5.7	Ave. 0	22.7*
4.2" Chemical Mortar Shell (HE) M3 (FT 4.2-B-1)					
	260	1.215	1.283	-	11.5
	395	1.200	1.384	-	1.4
	574	1.147	1.442	-	1.6
	716	1.047	1.349	-	4.0
	832	.932	1.225	-	0.9
Maximum variation % of average value		26.8	16.0	Ave. 0 (assumed)	3.9
81mm Mortar Shell M43 (FT 81-B-3)		(average for all elevations given in the FT)			
	235	1.127	1.178	16.5	3.8
	332	1.051	1.210	18.1	12.1
	419	0.904	1.032	8.5	14.2
	499	1.015	1.266	8.8	9.2
	572	0.932	1.104	13.6	19.0
	638	0.940	1.185	6.4	10.1
	700	0.863	1.152	8.1	3.9
Maximum variation % of average value		27.0	20.2	Ave 11.4	10.3
81mm Mortar Shell M56 (FT 81-C-2 and 81-C-3)					
	306	1.019	1.199	21.7	42.3
	412	.978	1.176	19.8	33.2
	502	.940	1.159	15.5	18.6
	582	.869	1.103	8.9	18.0
Maximum variation % of average value		15.8	8.3	Ave 16.5	28.0**

*Most of the variation of C_s with respect to change of elevation occurs for $\phi > 75°$. The values of C_s increase with increasing ϕ, indicating that the "average" air density decreased, as it should. That region had not been studied by means of the square law at the time of writing BRLM 434, in which the variation of C_s with ϕ was shown to be very small. Up to $\phi = 75°$ this variation, on the average, is only 9.4%. It needs hardly be mentioned that any data on the M49A2 shell at elevation >75° are not too reliable.

**Remarks similar to those of the preceding footnote apply to the M56 shell; up to $\phi = 75°$ the average variation of C_1 is 8.6% and of C_s 6.9%.

APPENDIX VI
GLOSSARY OF SYMBOLS

The notation used is for the most part consistent with that used in the Ordnance practice and in Cranz.

Consistent units are assumed, with one exception: symbols X and Z are reserved for the range and deflection expressed in yards; range and deflection in consistent units are denoted by X_c and Z_c.

The lower-case letters x, y, z, v, t and θ refer to the instantaneous values of the coordinates of the shell with respect to the muzzle (range, altitude and deflection to the right), velocity (with respect to ground), time of flight (from the exit from the muzzle) and inclination of the trajectory from the horizontal (reckoned upward), respectively. These letters are largely confined to Appendix I. In the integration formulas θ is expressed in radians.

Capitals X, Y, Z, V, T (and letters ϕ and ω) refer to terminal values of a trajectory; specifically,

V = muzzle velocity,

V_e = striking velocity;

X or X_c = range, with zero angle of sight (in yards or in consistent units, respectively);

Y is normally assumed to be zero;

ϕ = angle of departure (ordinarily, of elevation as well), degrees;

ω = angle of fall (reckoned positive), degrees.

Lower-case c = coefficient characterizing the retardation of the shell (cf. formulas 2 and 3').

Capital C without subscript = a parameter of the square-law trajectory (cf. Appendix I).

C_1, C_s, C_{sx}, C_{st} = ballistic coefficients of the shell, reckoned as is customary, cf. page11. Subscript 1 refers to the Gavre function, s to the square law. Subscripts x and t indicate whether the estimate of C_s was based on X or T; analogously with c_x and c_t.

g = acceleration of gravity; K_D = drag coefficient; i (with an appropriate subscript) = form-factor; m = mass of the shell; d (in inches or feet, according to context) = caliber of the shell.

$$\xi(\theta) = \int_0^\theta \sec^3\theta d\theta$$

β = arc $\xi(C)$, or $\xi(\beta) = C$.

$\eta = \sqrt{cV^2/g}$, an abbreviation used in charts (see formulas 2 and 2').

$\mu = 2gX_c/V^2$, an abbreviation used in charts (see formulas 4 and 4').

$\nu = 2cX_c$, an abbreviation used in charts (see formulas 5 and 5').

$\gamma = T\sqrt{gc}$, an abbreviation used in charts (see formulas 6 and 6').

$\zeta = 1/\sqrt{\mu}$, an abbreviation used in BRLM 434 (see Appendix II).

k_1, k_2, k_3 and k_4 = dimensionless derivatives (cf. page 9 and Appendix III).

W (with subscript x or z) = winds, assumed constant and small, and expressed in fps, positive forward and to the right.

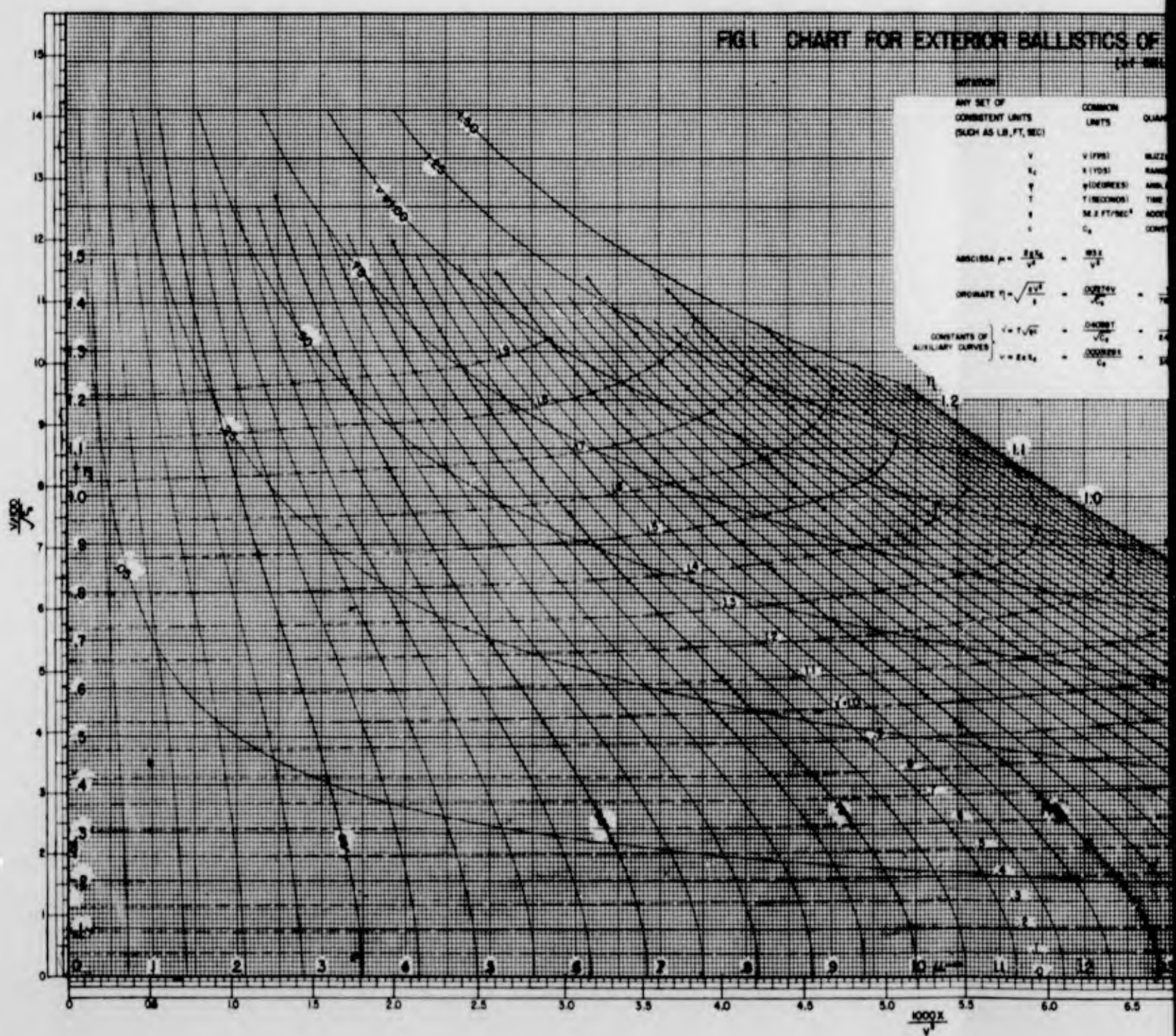
FIG I. CHART FOR EXTERIOR BALLISTICS OF
NOTATION
ANY SET OF CONSISTENT UNITS (SUCH AS LB, FT, SEC)
COMMON UNITS
V (FPS)
X (YDS)
φ (DEGREES)
T (SECONDS)
32.2 FT/SEC²
ABSCISSA μ =
ORDINATE η =
CONSTANTS OF AUXILIARY CURVES
1000 X / V²
1000 Y / X

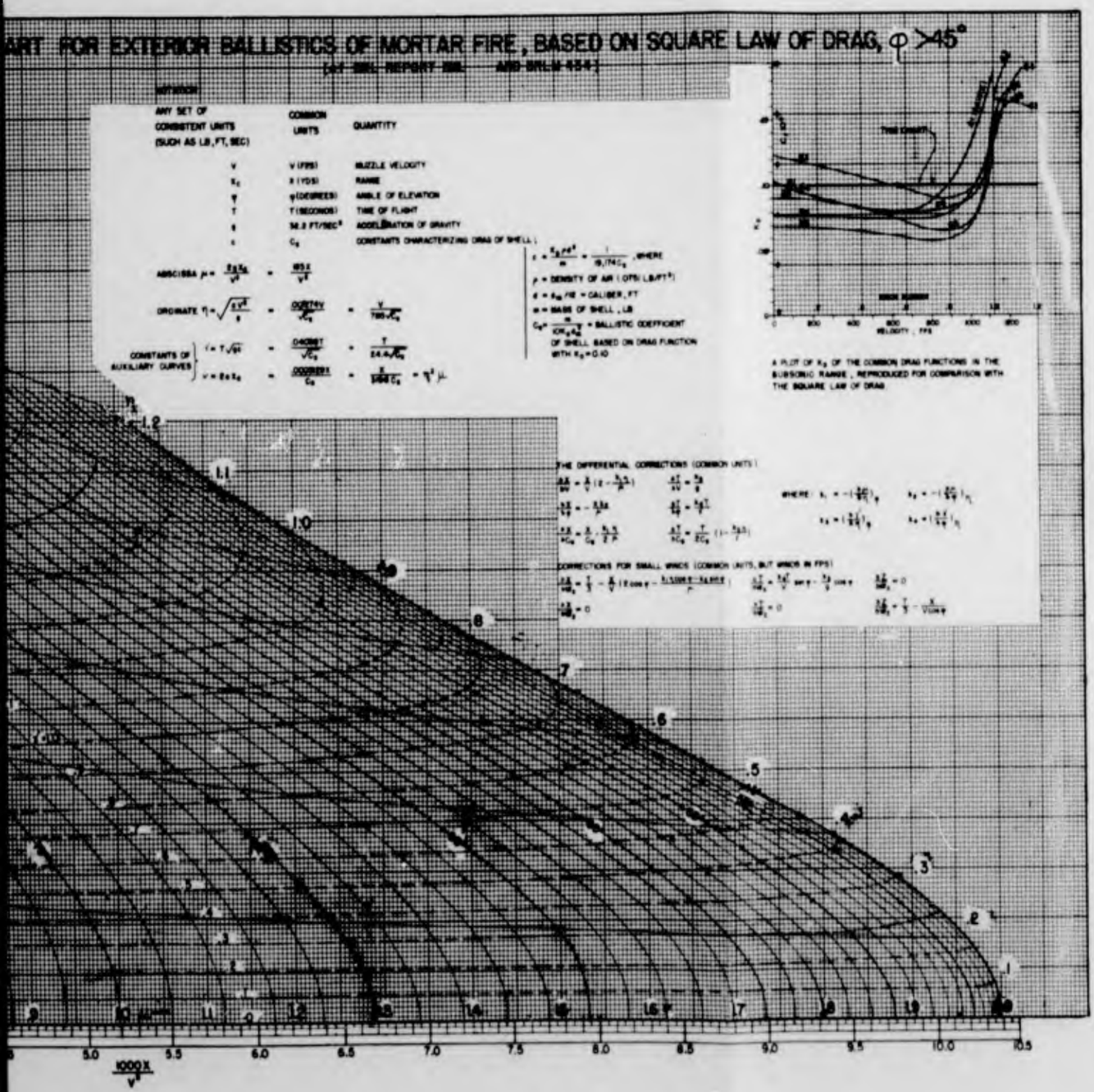
ART FOR EXTERIOR BALLISTICS OF MORTAR FIRE, BASED ON SQUARE LAW OF DRAG, φ >45°
NOTATION
ANY SET OF CONSISTENT UNITS (SUCH AS LB, FT, SEC)
COMMON UNITS
QUANTITY
V
V (FPS)
MUZZLE VELOCITY
x
X (YDS)
RANGE
φ
φ (DEGREES)
ANGLE OF ELEVATION
t
T (SECONDS)
TIME OF FLIGHT
g
32.2 FT/SEC²
ACCELERATION OF GRAVITY
i
CONSTANTS CHARACTERIZING DRAG OF SHELL
ABSCISSA
ORDINATE
CONSTANTS OF AUXILIARY CURVES
A PLOT OF i_y OF THE COMMON DRAG FUNCTIONS IN THE SUBSONIC RANGE, REPRODUCED FOR COMPARISON WITH THE SQUARE LAW OF DRAG
THE DIFFERENTIAL CORRECTIONS (COMMON UNITS)
CORRECTIONS FOR SMALL WINDS (COMMON UNITS, BUT WINDS IN FPS)
1.2
1.1
1.0
.9
.8
.7
.6
.5
.4
.3
.2
.1
5.0
5.5
6.0
6.5
7.0
7.5
8.0
8.5
9.0
9.5
10.0
10.5
1000 X / V²

2

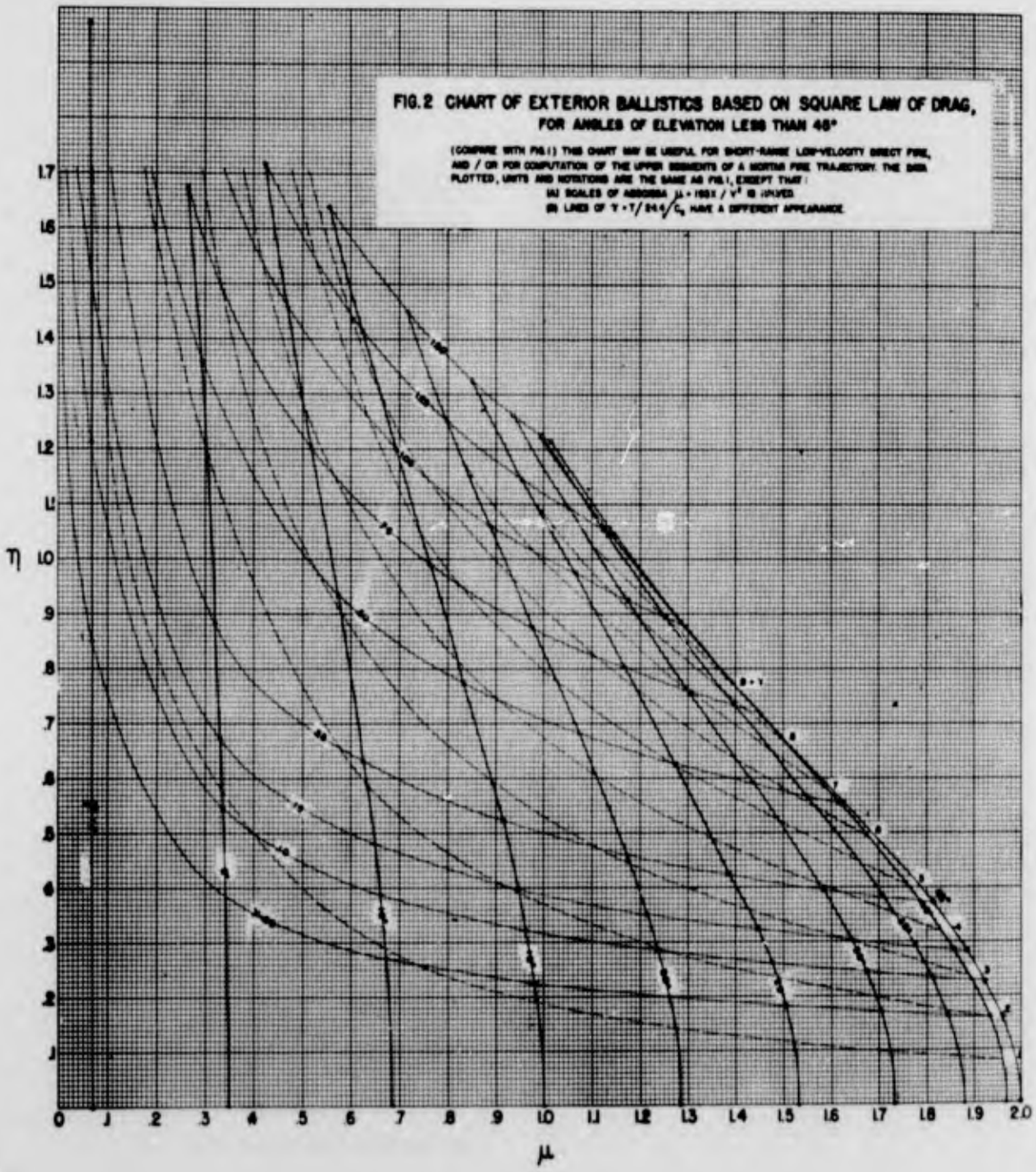
FIG. 2 CHART OF EXTERIOR BALLISTICS BASED ON SQUARE LAW OF DRAG,
FOR ANGLES OF ELEVATION LESS THAN 45°
η
μ
0
.1
.2
.3
.4
.5
.6
.7
.8
.9
1.0
1.1
1.2
1.3
1.4
1.5
1.6
1.7
1.8
1.9
2.0

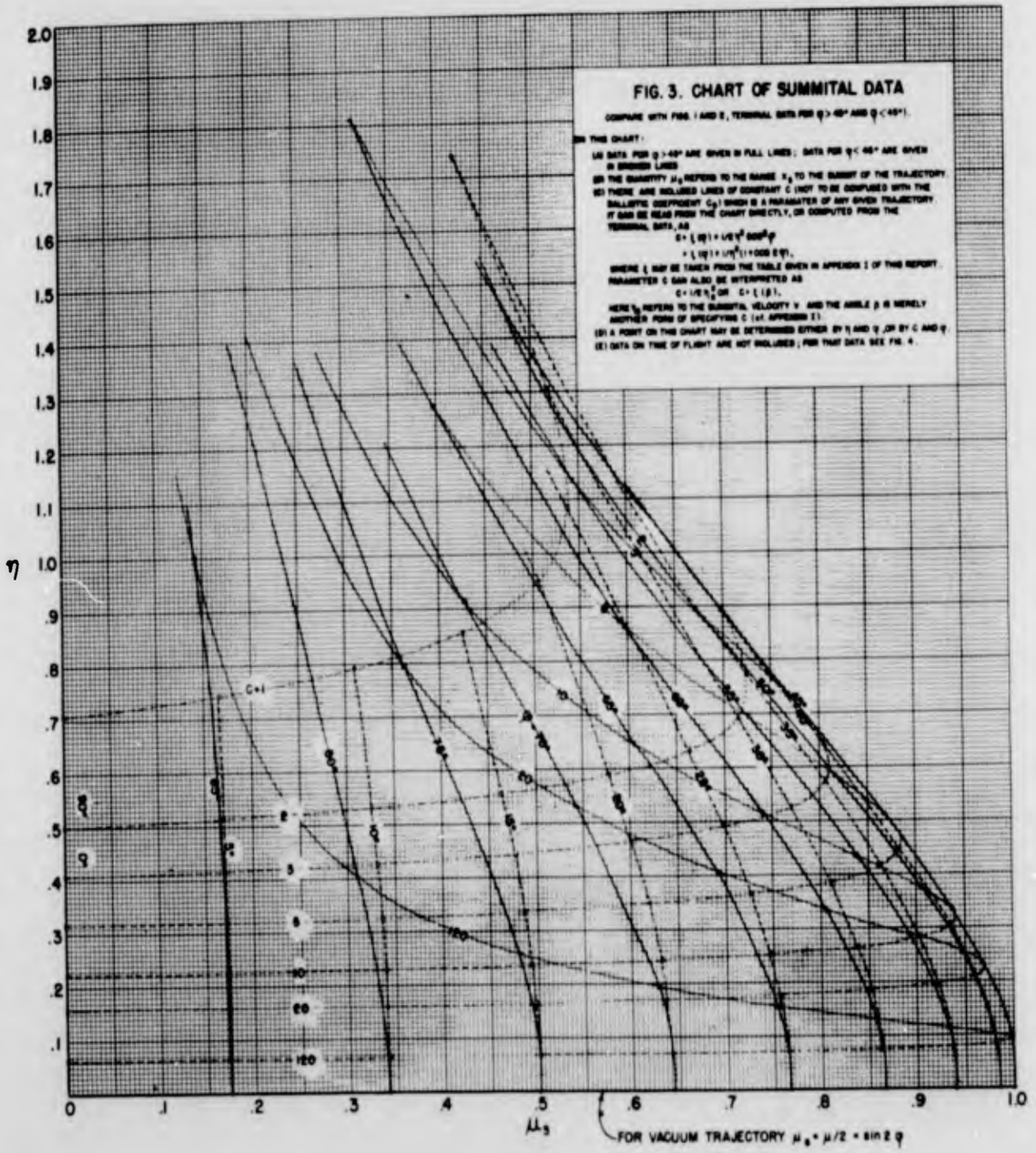
FIG. 3. CHART OF SUMMITAL DATA
η
μ_s
C=1
FOR VACUUM TRAJECTORY μ_s = μ/2 = sin 2φ

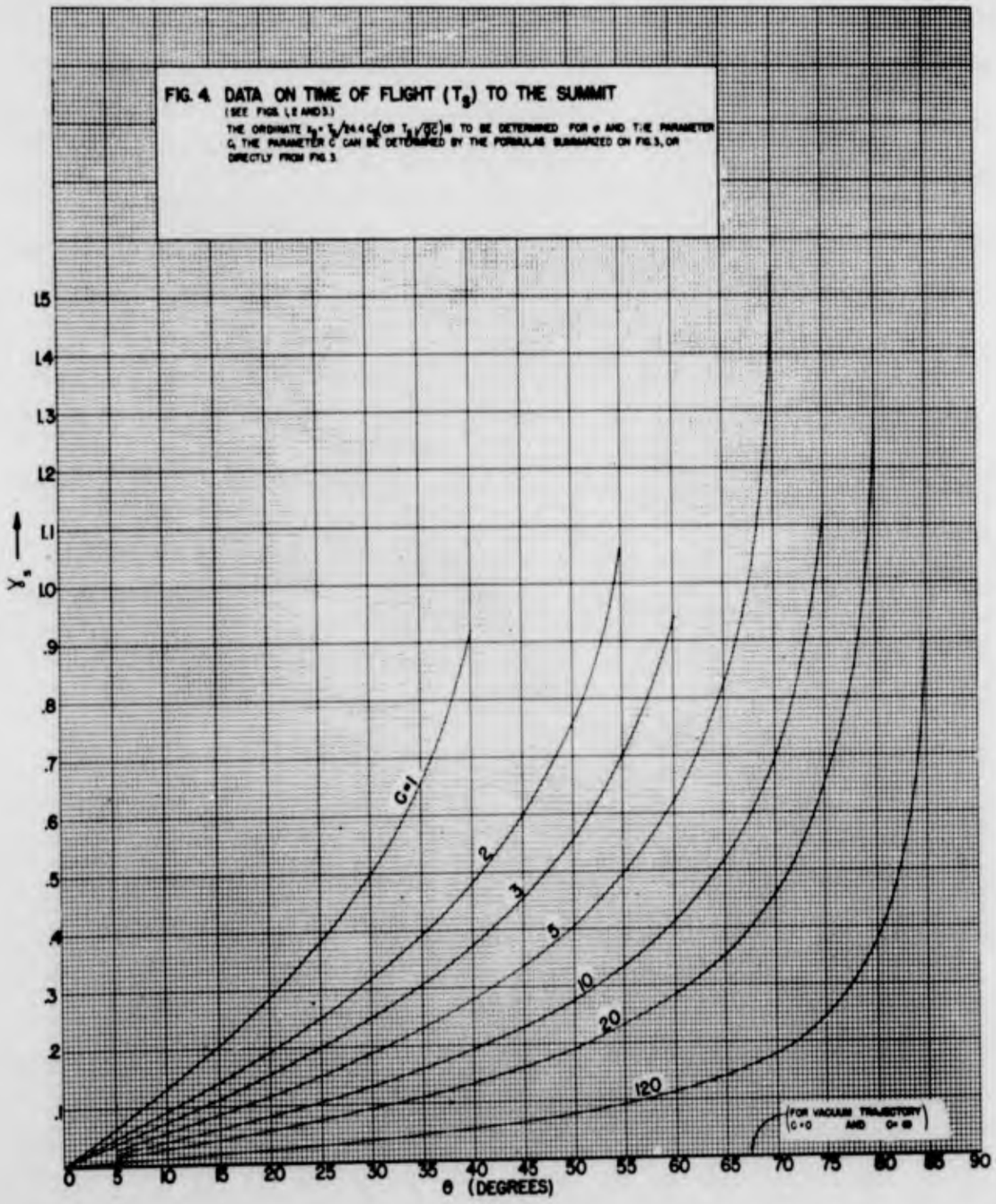
FIG. 4. DATA ON TIME OF FLIGHT (T_s) TO THE SUMMIT
(SEE FIGS. 1, 2 AND 3.)
THE ORDINATE $Y_s = T_s/24.4\,C_d$ (OR $T_s\sqrt{C_d}/24$) IS TO BE DETERMINED FOR φ AND THE PARAMETER C. THE PARAMETER C CAN BE DETERMINED BY THE FORMULAS SUMMARIZED ON FIG. 3, OR DIRECTLY FROM FIG. 3.
Y_s
1.5
1.4
1.3
1.2
1.1
1.0
.9
.8
.7
.6
.5
.4
.3
.2
.1
C=1
2
3
5
10
20
120
(FOR VACUUM TRAJECTORY C=0 AND C=∞)
0 5 10 15 20 25 30 35 40 45 50 55 60 65 70 75 80 85 90
θ (DEGREES)

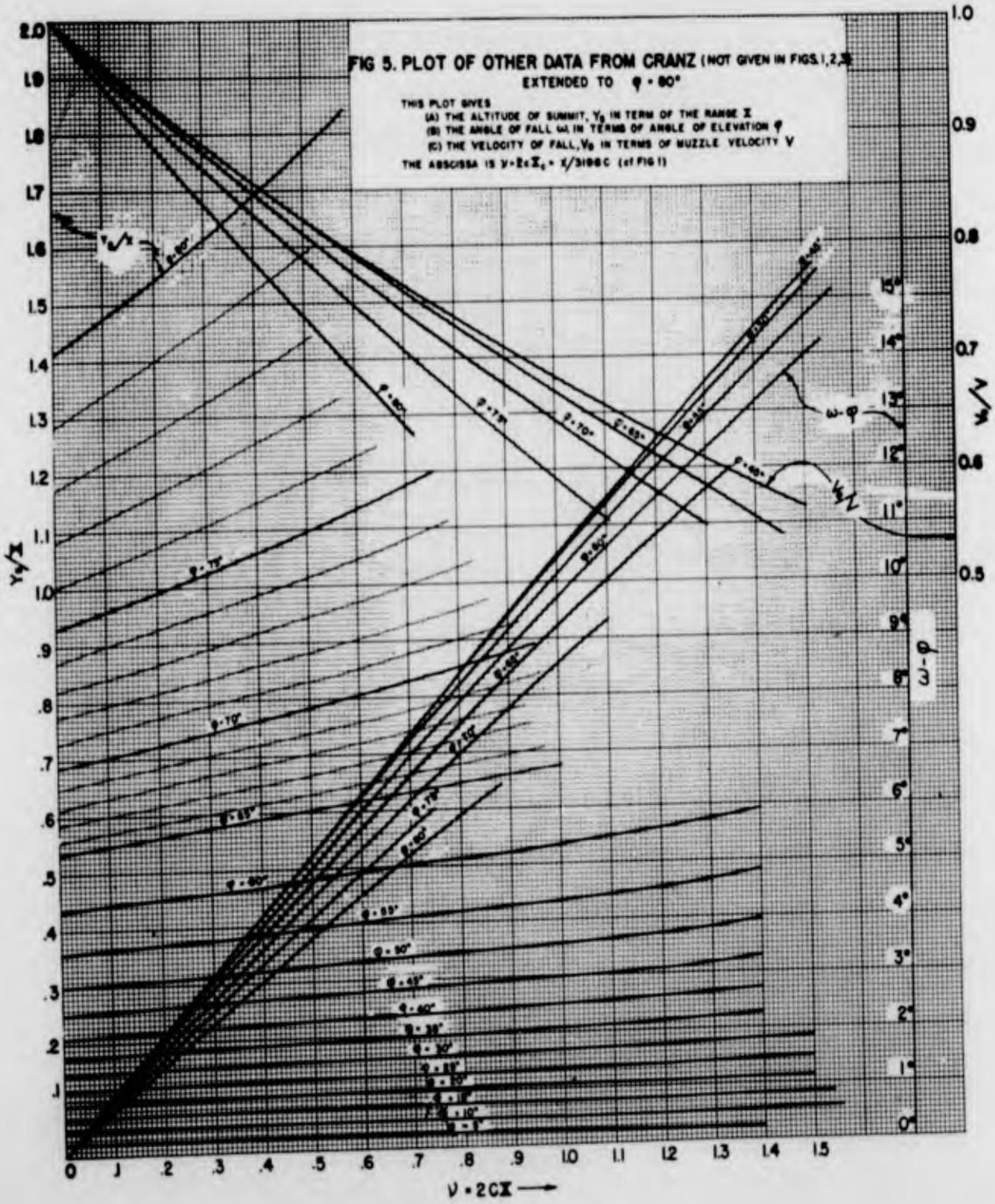
FIG 5. PLOT OF OTHER DATA FROM CRANZ (NOT GIVEN IN FIGS. 1, 2, 3)
EXTENDED TO φ = 80°
THIS PLOT GIVES
(A) THE ALTITUDE OF SUMMIT, Y_0 IN TERM OF THE RANGE Σ
(B) THE ANGLE OF FALL ω, IN TERMS OF ANGLE OF ELEVATION φ
(C) THE VELOCITY OF FALL, V_0 IN TERMS OF MUZZLE VELOCITY V
THE ABSCISSA IS $v = 2c\Sigma_0 = x/3100c$ (cf FIG 1)
Y_0/Σ
V/V_0
$\omega - \varphi$
$\frac{\varphi}{3}$
$v = 2c\Sigma \longrightarrow$

FIG. 6

A SAMPLE OF ESTIMATION OF TRAJECTORY

(CF LAST PAR. OF APPENDIX IV)

θ	η_θ	v	γ_s	$v-\gamma_s$	$2cy_s$	$2cy$	ω	$\frac{v_c}{v}$	η_c	γ	γ_s
$\varphi = 50.5^\circ$	.966	1.090	.592	.498	.409	.000	61.9°	.653	.631	1.268	.673
$\theta = 45^\circ$	.780	.845	.456	.389	.247	.162	53.9°	.723	.564	1.000	.482
30°	.553	.449	.233	.216	.070	.339	34.0°	.815	.451	0.539	.262
20°	.483	.271	.139	.132	.026	.383	21.4°	.878	.424	0.326	.160
(SUMMIT) 0°	.423	.000	.000	.000	.000	.409	00.0°	—	—	0.000	.000

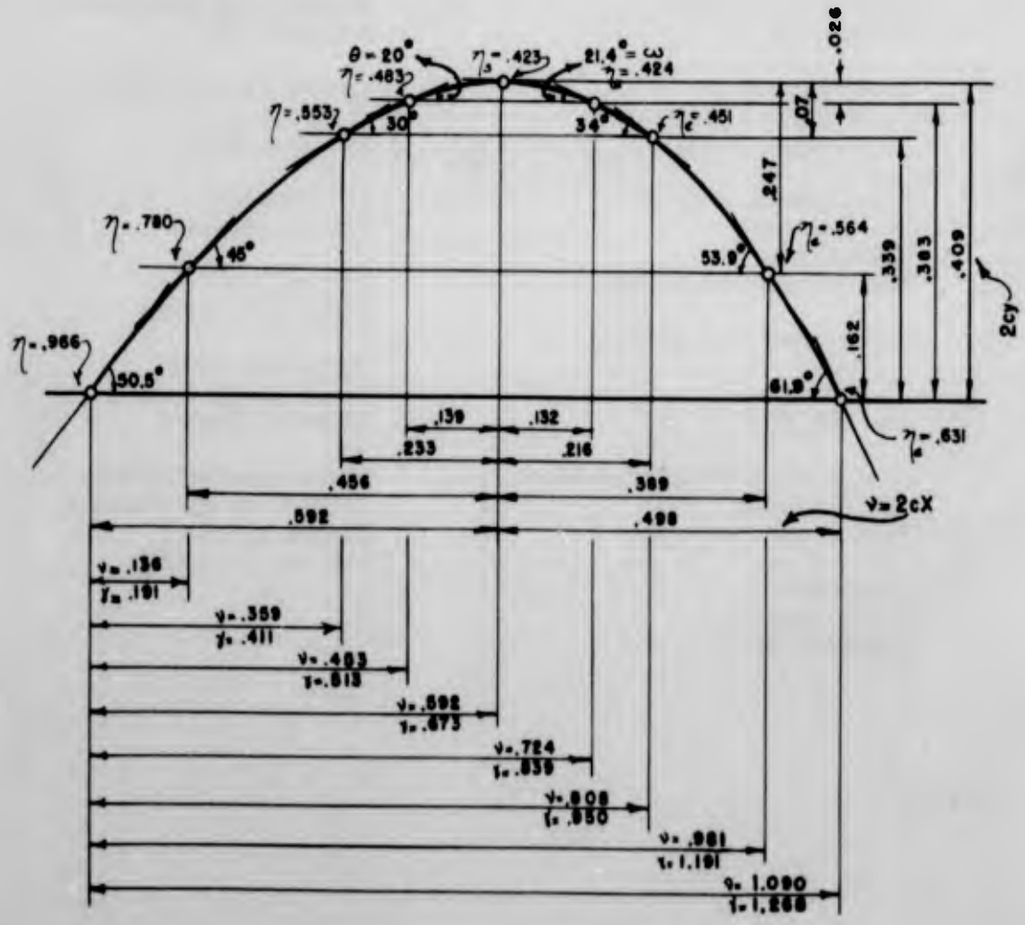

DISTRIBUTION LIST

No. of Copies		No. of Copies	
5	ORDTB - Bal Sec	2	National Bureau of Standards Washington, D.C. Attn: Mr. R. H. Heald Mr. Harry Diamond
10	British, of interest to Superintendent of External Ballistics Woolwich Arsenal	1	Sub-Office, OCO (Rocket) California Institute of Technology Pasadena, California
4	Chief, Bureau of Ordnance Washington 25, D.C. Attn: Re3	1	Commanding General, AGF Fort Monroe, Va. Attn: Development Section
2	Director Naval Ordnance Laboratory Washington 25, D.C.	1	President, AGF Board No. 1 Fort Bragg, N.C.
1	Commanding Officer Naval Proving Ground Dahlgren, Va.	1	President, AGF Board No. 4 Fort Bliss, Texas
1	Commanding Officer Naval Ordnance Test Station China Lake, California	1	AAA and GM Branch of Art. School Fort Bliss, Texas
1	Office Naval Research Navy Department Washington 25, D.C. Attn: Armament Br. (NR 463)	1	Artillery School Fort Sill, Oklahoma
1	Superintendent of Postgraduate School U.S. Naval Academy Annapolis, Md.	1	Infantry School Fort Benning, Georgia
1	Director, Naval Research Laboratory Anacostia Station Washington, D.C.	1	Commanding Officer Army Chemical Center Edgewood, Maryland
1	Commandant Marine Corps Washington 25, D.C.	1	Director, National Advisory Committee for Aeronautics Washington, D.C. Attn: Dr. H. L. Dryden

UNCLASSIFIED